Desalination and Water Treatment
www.deswater.com

doi: 10.5004/dwt.2020.24901

175 (2020) 164–173
January

Potential of natural clay derived functionalized adsorbent for the effective remediation of sanitary landfill leachate

K.Y. Foo

River Engineering and Urban Drainage Research Centre (REDAC), Engineering Campus, Universiti Sains Malaysia, 14300 Nibong Tebal, Penang, Malaysia, Tel. +6045996539; Fax: +6045996926; email: k.y.foo@usm.my

Received 25 April 2019; Accepted 11 September 2019

ABSTRACT

The management of landfill leachates, complex refractory wastewater which contains a host of organic pollutants, ammonia and degradation by-products, is a unique environmental challenge to the natural ecosystems. In this study, the preparation of a low-cost adsorbent from natural clay was implemented as a pre-treatment option for the adsorptive removal of chemical oxygen demand (COD) and ammonical-nitrogen from the semi-aerobic sanitary landfill leachate. The microstructure and surface chemistry were examined by porosity measurement, scanning electron microscopy and Fourier-transform infrared spectroscopy. Results manifested that the adsorptive removal of COD and ammonical-nitrogen was denoted at 71.93% and 68.94%, respectively, with a maximum monolayer adsorption capacity for COD and ammonical-nitrogen of 89.18 and 151.61 mg/g, respectively. The findings provided concrete evidence to support the potential of natural clay derived adsorbent as a prerequisite step on a large scale, for the innovative purification of highly contaminated landfill leachate.

Keywords: Adsorption; Functionalization; Isotherm; Kinetic; Landfill leachate; Natural clay

1. Introduction

During the past several decades, the exponential population growth, changes in productivity, consumption habits and resource use, have been accompanied by the rapid generation of municipal and industrial solid waste. In 1994, the global municipal solid waste production rate was reported at 1.3 billion tonnes per day, equivalent to an average of two-thirds of a kilogram per capita per day. In 2008, the figure has risen by 31.1%, designated a generation rate of 1.7 billion tonnes per day [1]. The disposal of municipal solid waste in sanitary landfills is recognized as the most common and desirable integral indispensable solid waste management practice, due to its simplicity of design, lower operating cost, and landscape-restoration of holes from mineral workings [2].

An important aspect related to the planning, operation and long-term management of municipal solid waste landfills is the generation of landfill leachate, and its subsequent contamination of the surrounding land and aquifers systems. This municipal solid waste would undergo physicochemical and biological changes; as a consequence of the decomposition of the organic fractions, along with the percolation of rainwater and moisture content, leading to the production of highly contaminated landfill leachate [3]. Under normal conditions, it would migrate down through the pores within the waste mass, and in modern containment landfills, it would drain away in the engineered drainage layer, to be collected at the lowest point in a sump or storage reservoir. Typically, the characteristic of the landfill leachate, can be best represented by chemical oxygen demand (COD), total organic carbon (TOC), biochemical oxygen demand (BOD_5), BOD_5/COD ratio, pH, suspended solids or ammonical-nitrogen (NH_3–N), that contains a broad variety of heavy metals, aromatic hydrocarbons, phenols, chlorinated aliphatic,

inorganic salts, recalcitrant compounds, anthropogenic chemicals, and other endocrine-disrupting constituents [4]. If poorly managed, the landfill leachate could become a major source of hydro-geological pollution for the receiving streams, creeks, water wells and the natural environment, to induce synergistic, toxicity, and genotoxicity [5].

Relatively, a couple of 100 hazardous compounds have been identified in the heterogeneous landfill leachate, by imposing a significant influence on the mobilization and attenuation towards the complexation of organic ligands and colloidal matters [6]. The adverse impacts of overloading in the sensitive ecosystems are becoming increasingly noticeable with several substances with confirmed carcinogenic or co-carcinogenic potential that were indicated in the landfill leachate, while others were expected to be persistent and highly bio-accumulative [7]. In recent decades, a wide range of new tertiary treatment processes for contaminant removal has abounded. Of major interest, adsorption is considered as the best treatment method, mainly hinges of its ease of operation, insensitivity to toxic substances and high removal capability, even from the dilute concentrations [8].

Despite its prolific use in water purification, the wide-scale implementation is deteriorated by the poor economic feasibility associated with the adsorbents manufacture and regeneration costs. In this sense, the call for an eco-friendly, cost-effective, industrially viable and renewable adsorbent would be an interesting strategy to lower the treatment cost, and enables the on-site remediation of landfill leachate [9]. Clay minerals, a member of the class of layered alumino-silicates, that make up the colloid fraction (<2 μm) of soils, sediments, rocks and water; or composed of a mixture of fine-grained minerals, crystals, quartz, carbonate and metal oxides, are ubiquitous present in nature [10]. It is characterized by a low hydraulic conductivity, high specific surface charges, and play an important role as a natural scavenger of water pollutants through ion exchange or adsorption processes [11]. Within this framework, the present work was undertaken towards the upgrading of the available natural clay into a low-cost, active functionalized adsorbent by chemical modifications for the innovative treatment of sanitary landfill leachate. The batch adsorption behavior was investigated as a prerequisite step on a large scale, for the on-site remediation of contaminated leachate samples. The structural, functional and surface chemistry of the prepared adsorbent was evaluated. The effects of adsorbent dosage loadings, contact time, and solution pH on the adsorption performance were evaluated. Moreover, the adsorption isotherms and kinetics are elucidated.

2. Materials and methods

2.1. Sanitary landfill leachate

The leachate samples were collected from a municipal waste sanitary landfill Pulau Burung landfill site (PBLS), located within the Byram Forest Reserve at 5°24′N, 100°24′E, in Penang, Malaysia. PBLS has been developed semi-aerobically into a Level II sanitary landfill employed a controlled tipping technique, and it was upgraded into a Level III sanitary landfill by controlled tipping with leachate recirculation system. The site has a natural marine clay liner with a total area of 33 ha, and is one of the only three sites of its kind in Malaysia.

The leachate samples were collected from the active detention pond with a leachate age of less than 5 years, and instantaneously transported to the laboratory, and stored in darkness at 4°C with minimum exposure to surrounding air as to minimize the chemical and biological changes. The mean characteristics of the leachate samples are presented in Table 1. The COD of the leachate varied between 1,810 and 2,850 mg/L, while the BOD_5 was less than 200 mg/L. Ammonia's strength, a major pollutant in the landfill leachate was identified to be 1,949 mg/L. Chemical analysis was performed according to the Standard Method of Water and Wastewater [12]. All experiments were undertaken in triplicates.

2.2. Natural clay derived functionalized adsorbent

Natural clay (NC) applied as a raw material in this work was procured locally. The raw precursor was washed exhaustively with deionized water to remove adhering dirt particles and water-soluble impurities from the surface. The clay was ground, sieved and screened to the desired mesh size of 1–2 mm. The clay micro-powder was mixed with 6 M of sulphuric acid solution at 75°C with occasional stirring at the stirring speed of 200 rpm for 4 h. The modified sample acid-modified natural clay (ANC) was rinsed repeatedly with hot and cold distilled water until the pH of the washing solution reached 6–7.

2.3. Physical and chemical characterizations

Scanning electron microscopy (SEM) was uniquely applied to identify a magnified, three-dimensional view of the modified clay surface with great depth of focus. The textural morphology was imaged using the Zeiss Supra 35 VP SEM (Carl Zeiss SMT, Oberköchen, Germany) equipped with W-Tungsten filament (Lanthanum-Hexaboride Field Emission), operated at 10–15 kV of speed voltage, 15 eV of resolution, and orientation of 35° with Mn Kα as the energy source.

The elemental compositions of natural clay and ANC were ascertained by energy-dispersive X-ray spectroscopy (EDX) analysis, which involves the generation of X-ray spectrum from the entire scan area of the SEM.

Table 1
Mean characteristics of the leachate samples

Parameter	Units	Measurement		Discharge limit
		Value	Average	
pH	–	8.30–9.17	8.58	6.0–9.0
COD	mg/L	1,810–2,850	2,321	400
NH_3–N	mg/L	1,630–2,200	1,949	5
Colour	Pt–Co	4,250–5,760	5,094	100
Turbidity	FAU	128–330	211	–
Suspended solid	mg/L	114–360	181	50
Conductivity	μS/cm	21,850–26,230	24,340	–

The pore structural characterization was determined by the nitrogen adsorption-desorption curve using an automatic Micromeritics ASAP-2020 volumetric adsorption analyzer (Micromeritics Inc., USA). A 21-point analysis was carried out at 77 K to obtain the nitrogen adsorption isotherm. The specific surface area (S_{BET}) was calculated by the Brunauer–Emmett–Teller (BET) equation; the total pore volume (V_T) was evaluated by converting the adsorption volume of nitrogen at relative pressure of 0.95 to equivalent liquid volume of the adsorbate, while the micropore volume, micropore surface area, and external surface area were deduced using the *t*-plot method. Chemical characterization of surface functional groups was detected using the pressed potassium bromide pellets containing 5% of carbon sample by Fourier-transform infrared spectrometer (FTIR-2000, PerkinElmer, Llantrisant, UK). The FTIR spectra were recorded from 4,000 to 400 cm^{-1}.

2.4. Batch adsorption studies

The batch adsorption experiments were carried out in a series of Erlenmeyer flasks containing 200 mL of leachate solution. The flasks were kept in an isothermal water bath shaker at 30°C with an agitation speed of 120 rpm. The samples were collected at prescribed time intervals. All samples were filtered using a syringe filter prior to analysis to minimize the interference of clay fines with the analysis. The adsorptive uptake of COD and ammonical-nitrogen (mg/g) at equilibrium q_e and time q_t were calculated by:

$$q_t = \frac{(C_0 - C_t)V}{W} \quad (1)$$

$$q_e = \frac{(C_0 - C_e)V}{W} \quad (2)$$

where C_0, C_t and C_e (mg/L) are the liquid-phase concentrations of COD and ammonical-nitrogen at initial, time *t* (min), and equilibrium, respectively. *V* is the volume of the solution (L), and *W* is the mass of adsorbent used (g). The pollutant removal (*R* %) was determined by:

$$R = \frac{(C_0 - C_e)}{C_0} \times 100\ \% \quad (3)$$

The analytical determination of COD and ammonical-nitrogen was conducted using the closed reflux colorimetric and nesslerization methods, with a visible spectrophotometer (HACH DR2500, HACH Company, Loveland, CO, USA).

3. Results and discussions

3.1. Effect of adsorbent dosage on the adsorptive uptake of COD and ammonical-nitrogen

Adsorbent dosage is the predominant variable affecting the adsorption process, due to the reason that it predicts the cost-effectiveness of the treatment system [13]. The retention of COD and ammonical-nitrogen to the variation of adsorbent dosage is depicted in Fig. 1. The adsorptive removal of COD and ammonical-nitrogen increased proportionally

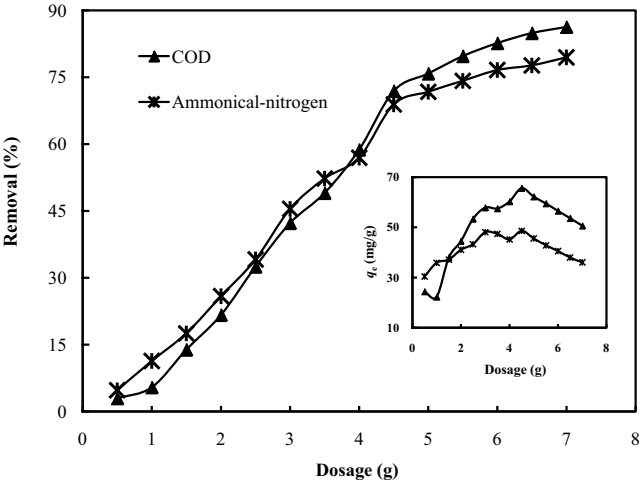

Fig. 1. Variation of adsorbent dosage on the adsorptive uptake and adsorptive removal of COD and ammonical-nitrogen onto ANC.

to the increase in adsorbent dosage from 0.5 g/200 mL to 4.5 g/200 mL. It is possible to suggest that by increasing the adsorbent dosage, there would be a greater availability of surface area and exchangeable binding sites for the entrapment of water pollutants. The optimum adsorptive uptake and adsorptive removal of COD and ammonical-nitrogen are denoted at 65.60 mg/g and 71.93%, and 48.62 mg/g and 68.94%, respectively.

Beyond the optimum dosage of 4.5 g/200 mL, there was no appreciable increase in the removal of COD and ammonical-nitrogen. Further increment in adsorbent dosage illustrated a slight decline of adsorptive uptake, consequence of the unsaturation of adsorption sites during the adsorption process. Additionally, higher adsorbent dosage could impose particle interaction, resulting from the aggregation and overcrowding of adsorbent particles. Such aggregation would lead to a decrease in the accessible surface area of ANC, lowering the pollutant removal per unit of adsorbent. The reduction in the adsorption capacity could be ascribed to the overlapping of the adsorption site as a result of overcrowding of adsorbent particles beyond 4.5 g/200 mL [14]. The statement was supported by the screening effect at a higher adsorbent dosage on the dense outer layer of the acid-activated natural clay, which shielding the binding sites from the COD and ammonium ions, lowering the COD and ammonical-nitrogen removal per unit of adsorbent.

3.2. Effect of contact time on the adsorptive uptake of COD and ammonical-nitrogen

The adsorptive uptake of COD and ammonical-nitrogen as a function of time, *t* was performed at the adsorbent dosage of 4.5 g/200 mL, and operating temperature of 30°C, as displayed in Fig. 2. Generally, the plots could be divided into three distinct regions: rapid adsorption during early stage, gradual adsorption till the equilibrium, and a plateau [15]. It is apparent from Fig. 2 that the adsorption process increased sharply at the initial stage, indicating the availability of readily accessible sites. The process was gradually

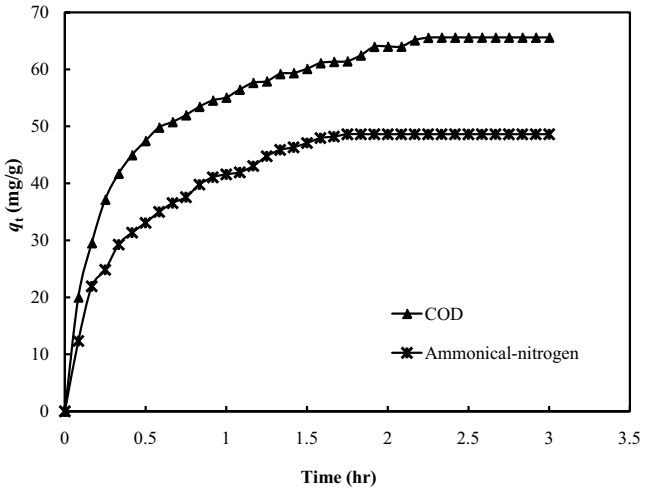

Fig. 2. Adsorptive uptake of COD and ammonical-nitrogen as a function of time.

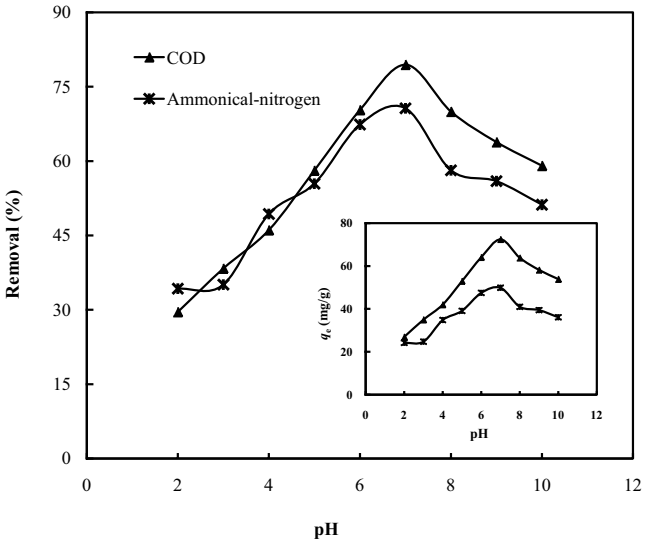

Fig. 3. Effect of solution pH on the adsorptive uptake of COD and ammonical-nitrogen.

slower, and the remaining vacant surface sites were difficult to be occupied due to the repulsive force between the solute molecules on the solid and bulk phases, as the equilibrium approached [16].

At this point, the COD and ammonium ions desorbing from the adsorbent is in a state of dynamic equilibrium with the amount of COD and ammonical-nitrogen being adsorbed onto the adsorbent. The time required to attain this state of equilibrium is termed as equilibrium time [17]. The amount of COD and ammonium ions adsorbed at equilibrium reflected the maximum adsorption capacity of the adsorbent under those operating conditions. Possibly, at the beginning, the solutes molecules were adsorbed onto the exterior surface of ANC. When the adsorption of the exterior surface reached to the saturation, the molecules need to diffuse into the interior surface. The time profile of COD and ammonical-nitrogen uptake is a single, smooth and continuous curve leading saturation, suggesting possible monolayer coverage of COD and ammonium ions onto the surface of ANC [18]. The adsorption equilibrium of COD and ammonical-nitrogen onto ANC was completed within 2.33 and 1.75 h, respectively. The contact time required for the leachate treatment process was relatively short, indicating its economical availability for the real practical applications.

3.3. Effect of solution pH on the adsorptive uptake of COD and ammonical-nitrogen

Solution pH is an important operational parameter affecting the degree of ionization and solubility of adsorbate, the concentration of the counterions, and surface charge of a solid adsorbent [19]. The adsorption behavior of COD and ammonical-nitrogen over a broad pH range of 2–10 is shown in Fig. 3. Generally, a stabilized leachate may contain a high amount of polar and nonpolar aggregated organic constituents, in the form of proteins, carbohydrates, detergents, lignin, tannins, fulvic acid, melanic acid, and humic acid, usually expressed in term of COD [20]. The extent of adsorption of these colored impurities depends primarily on their molecular weight, ionic charge, pH level, and hydrophobicity. The removal of these aggregation organic compounds may involve Van der Waals interactions between the non-ionic head and the hydrophobic matrix, and counterion displacement and electrostatic force between the positively charged quaternary ammonium functional group and negatively charged carboxylic or sulfonic groups [21].

Increasing the pH from 2 to 7 showed an enhancement of the adsorptive uptake for COD from 26.96 to 72.45 mg/g, and then it steadily decreased. The lower adsorption at a strong acidic pH of 2 to 4, can be attributed to the high mobility of H_3O^- ions competing with the organics cations for the adsorption sites. Similarly, it is likely that a strong electrostatic repulsion force presents between H_3O^- cations with the positively charged quaternary ammonium functional groups of adsorbent, leading to a sharp reduction of adsorption. In the basic medium of 8 to 10, the abundance of OH^- ion would induce a strong hindrance to the diffusion of organics anions. This interaction would mutually inhibit the adsorptive uptake of COD onto ANC [22]. Conversely, ammonical-nitrogen could present as NH_4^+ in the acidic condition (Eq. (4)), and present as NH_3 in the basic medium (Eq. (5)). It was clearly revealed that the adsorptive uptake of ammonical-nitrogen from the aqueous media increased by decreasing the solution pH from 12–7 with the presence of protons.

$$NH_3 + H_2O \leftrightarrow NH_4^+ + OH^- \quad (4)$$

$$NH_3 + H_3O^+ \leftrightarrow NH_4^+ + H_2O \quad (5)$$

$$NH_4^+ + OH^- \leftrightarrow NH_3 + H_2O \quad (6)$$

The presence of protons, arising from the displacement of equilibrium to the right (Eq. (6)) favors the Lewis acid–base interaction. However, at a strong acidic pH of 2 to 5, the presence excess of H_3O^- cations would introduce a strong

competitive effect to NH_4^+ cations for the surface actives sites to retard the adsorptive uptake of ammonical-nitrogen [23].

3.4. Adsorption isotherm

Adsorption equilibrium is established when an adsorbate containing phase has been contacted with the adsorbent for sufficient time, with its adsorbate concentration in the bulk solution is in a dynamic balance with the interface concentration. Adsorption isotherm is an invaluable data interpretation and predication that is essential for modeling analysis, operational design, and applicable practice of the adsorption systems [24]. Due to the inherent bias resulting from linearization, alternative isotherm parameter sets were determined by non-linear regression. This provides a mathematically rigorous method for determining the isotherm parameters using the original form of the isotherm equations. In the present work, the nonlinear Freundlich, Langmuir and Temkin isotherm models have been adopted.

Freundlich isotherm [25] is the earliest known relationship describing the non-ideal and reversible adsorption. This empirical model provides knowledge with regard to the surface heterogeneity and the exponential distribution of active sites, and their energies represented by:

$$q_e = K_F C_e^{1/n} \tag{7}$$

where K_F (mg/g) (L/mg)$^{1/n}$ and $1/n$ are the Freundlich adsorption constant, and a measure of adsorption intensity. Langmuir isotherm model, originally developed to describe gas–solid-phase adsorption systems, has been traditionally applied to quantify and contrast the performance of different bio-sorbents [26]. The model was formulated according to the fundamental assumptions that monolayer adsorption takes place at a finite number of localized sites, with each site holds homogeneity with the adsorbate molecules, and is energetically equivalent; with no interaction between the neighboring surfaces. The nonlinear form of the Langmuir isotherm model is written as:

$$q_e = \frac{Q_0 K_L C_e}{1 + K_L C_e} \tag{8}$$

where Q_0 (mg/g) and K_L (L/g) are the Langmuir isotherm constants related to adsorption capacity, and energy of adsorption. Temkin isotherm assumes that the adsorption heat of all the molecules in the layer would decrease linearly with surface coverage due to the adsorbate–adsorbent interactions [27]. The derivation is described by a uniform distribution of binding energies given by:

$$q_e = B \ln\left(AC_e\right) \tag{9}$$

where $B = RT/b$, and b (J/mol), A (L/g), R (8.314 J/mol K) and T (K) are the Temkin isotherm constant related to the heat of sorption, equilibrium binding constant, gas constant, and absolute temperature, respectively. The applicability of the isotherm models was carried out by judging the correlation coefficient, R^2 values, defined as:

$$R^2 = \frac{\left(q_{e,\text{meas}} - \bar{q}_{e,\text{calc}}\right)^2}{\sum\left(q_{e,\text{meas}} - \bar{q}_{e,\text{calc}}\right)^2 + \left(q_{e,\text{meas}} - \bar{q}_{e,\text{calc}}\right)^2} \tag{10}$$

where $q_{e,\text{meas}}$ and $q_{e,\text{calc}}$ are the measured and calculated concentration (mg/g), respectively, and $\bar{q}_{e,\text{calc}}$ is the average $q_{e,\text{calc}}$ (mg/g). The validity of the models to fit the data was further justified by the root-mean-squared errors (RMSE), the commonly used statistical tool measuring the predictive power of a model derived as:

$$\text{RMSE} = \sqrt{\frac{1}{N}\sum_{i=1}^{p}\left(\frac{\left(q_{i,\text{cal}} - q_{i,\text{exp}}\right)}{q_{i,\text{exp}}}\right)^2} \tag{11}$$

where $q_{i,\text{calc}}$ (mg/g) is the calculated amount of COD or ammonical-nitrogen that was adsorbed using the kinetics or isotherm adsorption models, $q_{i,\text{exp}}$ (mg/g) is the experimentally measured amount of adsorbed COD or ammonical-nitrogen, and N is the number of experimental data points.

The detailed parameters of these different forms of isotherm equations are listed in Table 2. The highest R^2 and lowest RMSE values reported in Table 2 showed a strong positive evidence that the adsorption of COD and ammonical-nitrogen onto ANC was best described by the Langmuir isotherm model, with a monolayer adsorption capacity for COD and ammonical-nitrogen of 89.18 and 151.61 mg/g, respectively. The best correlation with the Langmuir isotherm model indicated homogenous distribution of adsorbates molecules onto the active site of the ANC surface.

Table 2
Adsorption isotherm parameters for the adsorption of COD and ammonical-nitrogen onto ANC

Isotherms	Constants							
	COD				Ammonical-nitrogen			
Freundlich	n	K_F (mg/g) (L/mg)$^{1/n}$	R^2	RMSD	n	K_F (mg/g) (L/mg)$^{1/n}$	R^2	RMSD
	2.938	7.569	0.991	0.181	1.389	0.563	0.992	0.150
Langmuir	Q_0 (mg/g)	K_L (L/mg)	R^2	RMSD	Q_0 (mg/g)	K_L (L/mg)	R^2	RMSD
	89.178	4.79×10^{-3}	0.995	0.151	151.608	9.60×10^{-4}	0.994	0.139
Temkin	A (L/g)	B	R^2	RMSD	A (L/g)	B	R^2	RMSD
	0.046	19.981	0.987	0.231	0.011	30.522	0.989	0.162

A relatively well correlation coefficient, R^2 and RMSE values of the Freundlich isotherm model depicted the assertion that the adsorption of COD and ammonical-nitrogen onto ANC was not governed only by monolayer arrangement, but also by ion-exchange and complexation interactions via surface exchange mechanism. The value of $1/n$ measures the interactive relationship between the adsorbate molecules. The slope ranging between 0 and 1 is a measure of surface heterogeneity, a value below unity implies chemisorption, and above one is indicative of the cooperative adsorption. It was revealed that the adsorption intensity of the Freundlich isotherm model illustrated the value of $1/n$ is below the unity, indicating great feasibility of the chemisorption interactions. A comparison of the adsorption capacity of COD and ammonical-nitrogen onto different adsorbents is provided in Table 3. The adsorbent prepared in this work showed relatively high adsorption capacities for COD and ammonical-nitrogen of 89.18 and 151.61 mg/g, respectively, as compared to some previous works as reported in the literature. The current findings verified the capability of the ANC assisted adsorption process for the successful treatment of heavily polluted landfill leachate.

3.5. Adsorption kinetics

Generally, adsorption processes take place in a multistep mechanism (i) diffusion across the liquid film surrounding the solid particles (external mass transfer), (ii) diffusion within the particle (pore diffusion), and (iii) adsorption onto the surface binding sites. Adsorption kinetics provide an in-depth insight into the potential rate-controlling-steps, which in turn govern the mass transfer mechanism, residence time, efficiency of the adsorption process and feasibility of the scale-up operations [38]. The pseudo-first-order kinetic model [39], popularly known as the Lagergren rate expression, is described by:

$$\ln\left(\frac{q_e}{q_e - q_t}\right) = \frac{k_1}{2.303}t \tag{12}$$

where k_1 (1/h) is the pseudo-first-order kinetic rate constant. Contrary to the pseudo-first-order kinetic equation, pseudo-second-order kinetic equation [40] predicts the behavior over the whole range of adsorption. For the boundary conditions of $q_t = 0$ at $t = 0$ and $q_t = q_t$ at $t = t$, Ho's kinetic model is derived as:

$$\frac{1}{\left(q_e - q_t\right)} = \frac{1}{q_e} + k_2 t \tag{13}$$

where k_2 (g/mg h) is the pseudo-second-order kinetic rate constant. Elovich kinetic equation [41] is one of the most useful models describing the chemisorption process expressed by:

$$q_t = \frac{1}{b}\ln\left(ab\right) + \frac{1}{b}\ln t \tag{14}$$

where a (mg/g h) is the initial sorption rate, and b (g/mg) is related to the extent of surface coverage and activation energy for the chemisorption.

For interpretation of adsorption kinetics, the experimental data for the adsorption of COD and ammonical-nitrogen onto ANC at different time intervals were simulated by the pseudo-first-order, pseudo-second-order, and Elovich kinetic models, using the plots ln ($q_e - q_t$) against t, t/q_t vs. t, and q_t against ln t, respectively. The corresponding results are tabulated in Table 4. The suitability of the kinetic model to describe the adsorption process was ascertained by the value of correlation coefficient, R^2 and the normalized standard deviation, Δq (%) given by:

Table 3
Comparison of the adsorption capacities of COD and ammonical-nitrogen onto different adsorbents

Adsorbent	Adsorbate	Dosage	Monolayer adsorption capacity (mg/g)	References
Acid activated natural clay	COD	4.5 g/200 mL	89.18	Present study
Chinese loess	COD	0.1 g/50 mL	72.30	[28]
Ion exchange resin	COD	2 g/50 mL	39.84	[29]
Walnut shell activated carbon	COD	30 g/L	124.30	[30]
Composite	COD	50 g/100 mL	22.99	[31]
Zeolite	COD	50 g/100 mL	2.35	
Cow-dung ash	COD	20 g /L	53.19	[32]
Periwinkle shell activated carbon	COD	50 g/L	0.03	[33]
Commercial activated carbon	COD	50 g/L	0.08	
Acid activated natural clay	Ammonical-nitrogen	4.5g/200 mL	151.61	Present study
Sugarcane bagasse activated carbon	Ammonical-nitrogen	5 g/200 mL	138.46	[34]
Granular commercial clays	Ammonical-nitrogen	50 g/L	7.83	[35]
Modified clinoptilolite	Ammonical-nitrogen	1.5 g/L	2.03	[36]
Parthenocissus tricuspidata	Ammonical-nitrogen	0.2 g/25 mL	6.59	[37]
Coconut shell activated carbon	Ammonical-nitrogen	33.3 g/L	17.19	[23]

$$\Delta q\ (\%) = 100\sqrt{\frac{\sum\left|\left(q_{e,\exp} - q_{e,\mathrm{calc}}\right)/q_{e,\exp}\right|^2}{N-1}} \quad (15)$$

where $q_{e,\exp}$ (mg/g) and $q_{e,\mathrm{calc}}$ (mg/g) are the experimental and calculated adsorption capacities, respectively. The correlation coefficient obtained for the pseudo-first-order and Elovich kinetic models were relatively small, and the experimental q_e values did not agree satisfactory with the calculated values. Good agreement was shown between the experimental data with the pseudo-second-order kinetic model, with the $R^2 > 0.99$, and the lowest normalized standard deviation, Δq (%) values of 1.32% and 2.99%. This observation suggested that the adsorption system followed the pseudo-second-order kinetic model, based on the assumption that the rate-limiting step may be chemisorption rather than diffusion-controlled, which involves valency forces through electrons sharing between ANC and the adsorbate molecules.

3.6. Physical and chemical characterizations

The surface morphology of the natural clay and ANC was visualized via SEM, with the magnification of 2,000 X as shown in Fig. 4. The morphology of the natural clay was very fine, irregular, with the presence of curved flakes and mats of coalesced flakes. Generally, these flakes seem to be anhedral, but it was difficult to determine their exact texture due to the particle coalescence. Examination of the SEM micrographs demonstrated that these particles were smaller and thinner after acid modification, with a well developed porous structure, indicating the good possibility for the pollutants to be trapped.

The result of the EDX provided a clear verification of the changes in the clay compositions following acid modification. The natural clay sample contained predominantly a mixture of carbon (C), oxygen (O), iron (Fe), copper (Cu), sodium (Na), magnesium (Mg), aluminium (Al), silica (Si), and potassium (K), with the weight fraction of 7.06%, 41.36%, 3.19%, 0.36%, 0.18%, 0.22%, 16.60%, 28.82%, and 2.21% respectively. Nevertheless, acid modification dictated a drastically increase of carbon (12.75%) and silica (35.95%) content, while the compositions of oxygen (30.66%), iron (2.21%), copper (0.2%), sodium (0.13%), magnesium (0.19%), aluminium (16.01), and potassium (1.9%) were slightly decreased.

Nitrogen adsorption–desorption analysis is a standard protocol for the determination of the porosity of the solid adsorbents [42]. The surface physical parameters obtained from the N_2 adsorption isotherms are listed in Table 5.

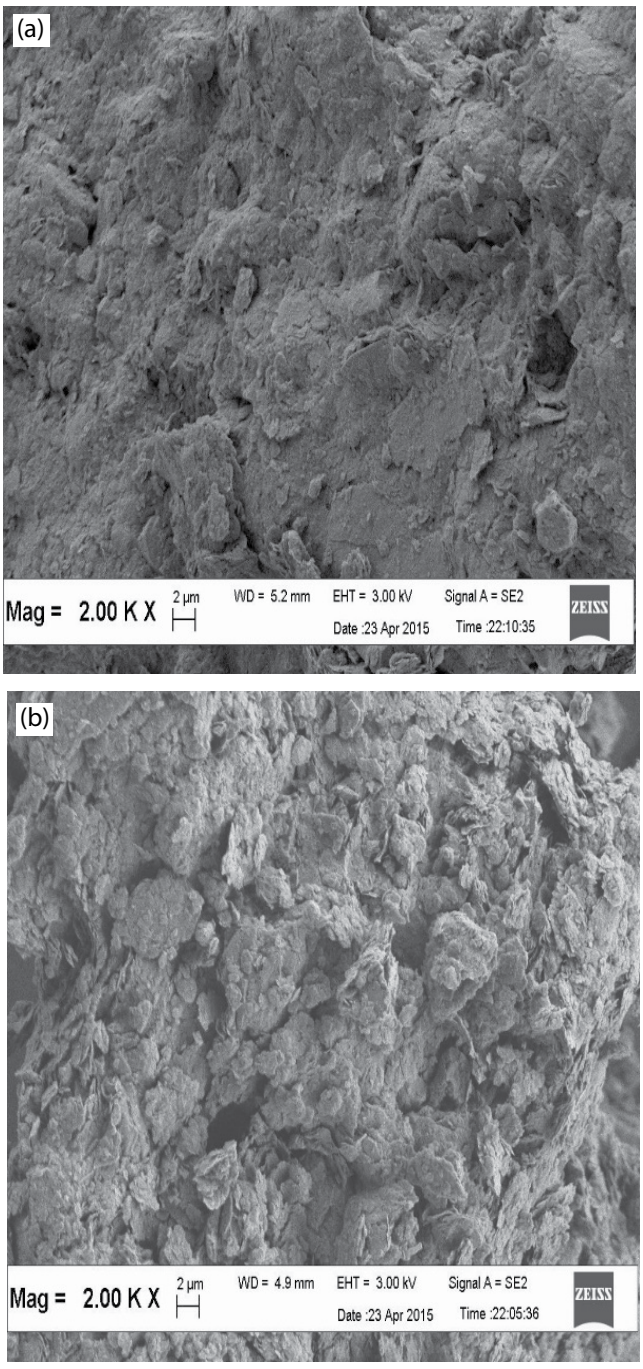

Fig. 4. Surface morphology of the natural clay and ANC.

Table 4
Adsorption kinetic parameters for the adsorption of COD and ammonical-nitrogen onto ANC

Adsorbate	$q_{e,\exp}$ (mg/g)	Pseudo-first-order				Pseudo-second-order				Elovich				
		k_1 (1/h)	$q_{e,\mathrm{calc}}$ (mg/g)	R^2	Δq (%)	k_2 (g/mg)	$q_{e,\mathrm{calc}}$ (mg/g)	R^2	Δq (%)	a (mg/g h)	B (g/mg)	$q_{e,\mathrm{calc}}$ (mg/g)	R^2	Δq (%)
COD	65.60	3.545	43.13	0.971	34.25	0.071	67.57	0.998	2.99	692.20	0.068	69.16	0.993	5.42
Ammonical-nitrogen	48.62	3.901	36.83	0.974	24.24	0.086	49.26	0.997	1.32	427.91	0.088	47.47	0.994	2.36

Table 5
Surface physical parameters of ANC

Properties	Natural clay	ANC
BET surface area (m^2/g)	10.37	102.31
Micropore surface area (m^2/g)	4.90	26.05
External surface area (m^2/g)	5.47	76.26
Langmuir surface area (m^2/g)	13.59	152.73
Total pore volume (cm^3/g)	0.004	0.058
Micropore volume (cm^3/g)	0.001	0.017
Mesopore volume (cm^3/g)	0.003	0.041
Average pore size (nm)	3.286	2.250

Table 6
Characteristics of the FTIR bands for natural clay and ANC

IR peak	Wavenumber (cm^{-1})		Band assignment
	Natural clay	ANC	
1	3,699	3,698	(–OH) group stretching
2	3,628	3,621	Hydration, (–OH) group stretching
3	1,637	1,627	Hydration, HOH deformation
4	1,010	1,008	(Si–O) group stretching
5	912	910	OH deformation, linked to $2Al^{2+}$
6	780	779	OH deformation, linked to Al^{3+} and Mg^{2+}
7	538	535	(Si–O–Al), SiO deformation and AlO stretching
8	469	467	(Si–O–Si), SiO deformation and SiO stretching

The BET surface area, Langmuir surface area and total pore volume of ANC were identified to be 102.31 m^2/g, 152.73 m^2/g, and 0.058 m^3/g, respectively. Conversely, the raw natural clay demonstrated the low BET surface area, Langmuir surface area, and total pore volume of 10.37 m^2/g, 13.59 m^2/g, and 0.004 cm^3/g, respectively, implying pore development and widening of the existing pores during the acid modification stage. The mesopores of ANC account for approximately 71% of the total pore volume, indicating its great feasibility for the water purification applications.

The representative transmission spectra of natural clay and ANC are displayed in Table 6. The FTIR spectra illustrated the presence of smectite as a dominant mineral phase. The IR band at 3,699/3,698 cm^{-1} is attributed to the stretching vibrations of OH group associated with cations. The region between 3,628/3,821 and 1,637/1,627 cm^{-1} showed the stretching and deformation vibrations, related to the –OH groups of the interlayer water molecules. The signal at 1,010/1,008 cm^{-1} is assigned to the Si–O peak group, while the dissolution of the octahedral sheets showed a sharp peak corresponding to the –OH bending, linked to (AlAlOH) at 912/910 cm^{-1}. The almost full disappearance of the wideband at 780/799 cm^{-1} is identical to AlMgOH, pointing out to the significant leaching of the Mg yield by acid modification, and the intensities at 538/535 and 469/467 cm^{-1} are ascribed to the deformation of Si–O–Al and Si–O–Si, respectively. The reduction of the corresponding bands at 3,699; 1,010; 538; and 469 cm^{-1} and a significant decrease, almost disappearance of the signal at 3,628 cm^{-1} depicted the continuous release, and significant leaching of the octahedral cations during the acid treatment process.

The results implied that acid modification has induced a corrosive implication on the octahedral sheet of the natural clay, accompanied by the release of Al^{3+} and other cation species from both tetrahedral and octahedral sites, while the SiO_4 and SiO_3OH groups of the tetrahedral sheet stayed largely intact. Meanwhile, the crystalline structure of the natural clay has transformed the amorphous structure, leading to the formation of additional Al–OH and Si–OH bonds [43,44]. Besides, the central atoms from the octahedral and tetrahedral Al were removed from the clay mineral to be substituted, subsequent by the partial dissolution of tetrahedral and octahedral sheets, with the formation of new acid sites. These alterations of the surface chemistry, together with the morphological development, and tremendous improvement of the porosity structure have justified the higher stability and flexibility of the tetrahedral sheets to enhance its adsorptive capability.

4. Conclusion

In this work, laboratory experiments were undertaken to investigate a natural clay derived adsorbent for the successful treatment of sanitary landfill leachate. The prepared adsorbent attained the BET surface area of 102.31 m^2/g, and a high contribution of mesopores of 75%. Langmuir isotherm model provided the best fit to the experimental data, with a maximum monolayer adsorption capacity for COD and

ammonical-nitrogen of 89.18 and 151.61 mg/g, respectively. The findings revealed a new entry for the pretreatment of landfill leachate featured by operational simplicity, low-cost, high efficiency, and eco-friendly due to the renewable-utilization of waste to treat hazardous waste. The spent natural clay-based green adsorbent may be integrated as fertilizers or soil conditioners in different agricultural systems, with better soil-deliverability, controlled nutrient release, higher biocompatibility, and nutrient reuse efficiency.

Acknowledgment

The authors acknowledge the financial support provided by Universiti Sains Malaysia, under the USM Short Term Grant Scheme (Project No. 304/PREDAC/6315111).

References

[1] S. Renou, J.G. Givaudan, S. Poulain, F. Dirassouyan, P. Moulin, Landfill leachate treatment: review and opportunity, J. Hazard. Mater., 150 (2008) 468–493.
[2] M.D. Vaverková, J. Winkler, D. Adamcová, M. Radziemska, D. Uldrijan, J. Zloch, Municipal solid waste landfill – vegetation succession in an area transformed by human impact, Ecol. Eng., 129 (2019) 109–114.
[3] W.J. Yin, K. Wang, D.J. Wu, J.T. Xu, X.R. Gao, X.X. Cheng, C.W. Luo, C.C. Zhao, Variation in bacterial communities during landfill leachate treatment by a modified sequencing batch reactor (SBR), Desal. Wat. Treat., 140 (2019) 365–372.
[4] K.Y. Foo, L.K. Lee, B.H. Hameed, Batch adsorption of semi-aerobic landfill leachate by granular activated carbon prepared by microwave heating, Chem. Eng. J., 222 (2013) 259–264.
[5] N.C. de Almeida, A.U. de Faria, V.J.A. de Oliveira, J.S. Govone, D. de Franceschi de Angelis, Biodegradation and toxicity of byproducts from the treatment of landfill leachate with hydrotalcite, Desal. Wat. Treat., 118 (2018) 281–293.
[6] D.L. Jensen, T.H. Christensen, Speciation of Heavy Metals in Landfill-Leachate, Proc. Sardinia'97, 6th International Landfill Symposium, Italy, 1997, pp. 161–168.
[7] C. Qi, G. Yu, M. Zhong, G. Peng, J. Huang, B. Wang, Organophosphate flame retardants in leachates from six municipal landfills across China, Chemosphere, 218 (2019) 836–844.
[8] D. Suteu, G. Biliuta, L. Rusu, S. Coseri, C. Vial, I. Nica (Nebuna), A regenerable microporous adsorbent based on microcrystalline cellulose for organic pollutants adsorption, Desal. Wat. Treat., 146 (2019) 176–187.
[9] K.Y. Foo, L.K. Lee, B.H. Hameed, Preparation of tamarind fruit seed activated carbon by microwave heating for the adsorptive treatment of landfill leachate: a laboratory column evaluation, Bioresour. Technol., 133 (2013) 599–605.
[10] M.K. Uddin, A review on the adsorption of heavy metals by clay minerals, with special focus on the past decade, Chem. Eng. J., 308 (2017) 438–462.
[11] S.F.A. Shattar, N.A. Zakaria, K.Y. Foo, Feasibility of montmorillonite-assisted adsorption process for the effective treatment of organo-pesticides, Desal. Wat. Treat., 57 (2016) 13645–13677.
[12] APHA, AWWA, WPCF, Standard Methods for the Examination of Water and Wastewater, 18th ed., American Public Health Association, Washington, D.C., USA, 1992.
[13] M.E. Bidhendi, M.A. Gabris, V. Goudarzi, S. Abedynia, B.H. Juma, H. Sereshti, M.A. Kamboh, M. Soylak, H.R. Nodeh, Removal of some heavy metal ions from water using novel adsorbent based on iron oxide-doped sol-gel organic-inorganic hybrid nanocomposite: equilibrium and kinetic studies, Desal. Wat. Treat., 147 (2019) 173–182.
[14] K. Moodley, R. Singh, E.T. Musapatika, M.S. Onyango, A. Ochieng, Removal of nickel from wastewater using an agricultural adsorbent, Water SA, 37 (2011) 41–46.
[15] K.Y. Foo. Preparation of eco-friendly activated carbon as a refining solution for the adsorptive treatment of analgesic acetaminophen, Desal. Wat. Treat., 114 (2018) 332–340.
[16] I. Kipcak, C. Akin, Cadmium removal from aqueous solution by iron oxide coated sepiolite: preparation, characterization and batch adsorption studies, Desal. Wat. Treat., 146 (2019) 245–256.
[17] K.Y. Foo, L.K. Lee, B.H. Hameed, Preparation of banana frond activated carbon by microwave induced activation for the removal of boron and total iron from landfill leachate, Chem. Eng. J., 223 (2013) 604–610.
[18] M. Dinari, A. Haghighi, P. Asadi, Facile synthesis of ZnAl-EDTA layered double hydroxide/poly(vinyl alcohol) nanocomposites as an efficient adsorbent of Cd(II) ions from the aqueous solution, Appl. Clay Sci., 170 (2019) 21–28.
[19] V. Gascóna, A. Arencibiab, J.M. Arsuagab, Efficient amine-SBA-15-type adsorbents for treatment of water containing trace levels of Pb(II) and Cd(II), Desal. Wat. Treat., 146 (2019) 210–226.
[20] K.Y. Foo, B.H. Hameed, An overview of landfill leachate treatment via activated carbon adsorption process, J. Hazard. Mater., 171 (2009) 54–60.
[21] Y.R. Tan, J.E. Kilduff, Factor affecting selectivity during dissolved organic matter removal by anion-exchange resins, Water Res., 41 (2007) 4211–4221.
[22] J. Rodríguez, L. Castrillón, E. Marañón, H. Sastre, E. Fernández, Removal of nonbiodegradable organic matter from landfill leachates by adsorption, Water Res., 38 (2004) 3297–3303.
[23] X.L. Long, H. Cheng, Z.L. Xin, W.D. Xiao, W. Li, W.K. Yuan, Adsorption of ammonia on activated carbon from aqueous solutions, Environ. Prog., 27 (2008) 225–233.
[24] K.Y. Foo, B.H. Hameed, Insights into the modeling of adsorption isotherm systems, Chem. Eng. J., 156 (2010) 2–10.
[25] H.M.F. Freundlich, Over the adsorption in solution, J. Phys. Chem., 57 (1906) 385–471.
[26] L. Langmuir, The constitution and fundamental properties of solids and liquids, J. Am. Chem. Soc., 38 (1916) 2221–2295.
[27] M.I. Tempkin, V. Pyzhev, Kinetics of ammonia synthesis on promoted iron catalyst, Acta Phys. Chim. USSR, 12 (1940) 327–356.
[28] H. Xie, S. Wang, Z. Qiu, J. Jiang, Adsorption of NH_4^+–N on Chinese loess: non-equilibrium and equilibrium investigations, J. Environ. Manage., 202 (2017) 46–54.
[29] W. Sun, D. Yue, J. Song, Y. Nie, Adsorption removal of refractory organic matter in bio-treated municipal solid waste landfill leachate by anion exchange resins, Waste Manage., 81 (2018) 61–70.
[30] A.R. Mahdavi, A.A. Ghoresyhi, A. Rahimpour, H. Younesi, K. Pirzadeh, COD removal from landfill leachate using a high-performance and low-cost activated carbon synthesized from walnut shell, Chem. Eng. Commun., 205 (2018) 1193–1206.
[31] A.A. Halim, H.A. Aziz, M.A.M. Johari, K.S. Ariffin, Comparison study of ammonia and COD adsorption on zeolite, activated carbon and composite materials in landfill leachate treatment, Desalination, 262 (2010) 31–35.
[32] K. Kaur, S. Mor, K. Ravindra, Removal of chemical oxygen demand from landfill leachate using cow-dung ash as a low-cost adsorbent, J. Colloid Interface Sci., 469 (2016) 338–343.
[33] M.A.O. Badmus, T.O.K. Audu, Periwinkle shell: based granular activated carbon for treatment of chemical oxygen demand (COD) in industrial water, Can. J. Chem. Eng., 87 (2009) 69–77.
[34] K.Y. Foo, L.K. Lee, B.H. Hameed, Preparation of activated carbon from sugarcane bagasse by microwave assisted activation for the remediation of semi-aerobic landfill leachate, Bioresour. Technol., 134 (2013) 166–172.
[35] R.S.D.P. Couto, A.F. Oliveira, A.W.S. Guarino, D.V. Perez, M.R.D.C. Marques, Removal of ammonia nitrogen from distilled old landfill leachate by adsorption on raw and modified aluminosilicate, Environ. Technol., 38 (2017) 816–826.
[36] H.X. Huo, H. Lin, Y.B. Dong, H. Cheng, H. Wang, L.X. Cao, Ammonia-nitrogen and phosphate sorption from stimulated reclaimed waters by modified clinoptilolite, J. Hazard. Mater., 134 (2012) 166–172.

[37] H.W. Liu, Y.H. Dong, H.Y. Wang, Y. Liu, Adsorption behaviour of ammonium by a bioadsorbent – Boston ivy leaf powder, J. Environ. Sci., 22 (2010) 1513–1518.
[38] M. Sattar, F. Hayeeye, W. Chinpa, O. Sirichote, Poly(lactic acid)/activated carbon composite beads by phase inversion method for kinetic and adsorption studies of Pb^{2+} ions in aqueous solution, Desal. Wat. Treat., 146 (2019) 227–235.
[39] S. Langergren, B.K. Svenska, Zur theorie der sogenannten adsorption geloester stoffe, Veternskapsakad Handlingar, 24 (1898) 1–39.
[40] Y.S. Ho, Adsorption of Heavy Metals from Waste Streams by Peat, Ph.D. Dissertation, University of Birmingham, Birmingham, UK, 1995.
[41] C. Aharoni, F.C. Tompkins, Kinetics of Adsorption and Desorption and the Elovich Equation, D.D. Eley, H. Pines, P.B. Weisz, Eds., Advances in Catalysis, Vol. 21, Academic Press, New York, 1970, pp. 1–49.
[42] K.Y. Foo, Effect of microwave regeneration on the textural network, surface chemistry and adsorptive property of the agricultural waste based activated carbons, Process Saf. Environ. Prot., 116 (2018) 461–467.
[43] G. Suraj, C.S.P. Iyer, M. Lalithambika, Adsorption of cadmium and copper by modified kaolinite, Appl. Clay Sci., 13 (1998) 293–306.
[44] S.F.A. Shattar, N.A. Zakaria, K.Y. Foo, Enhancement of hazardous pesticide uptake, ametryn using an environmentally friendly clay-based adsorbent, Desal. Wat. Treat., 79 (2017) 188–195.